演題 3

前頭側頭型認知症を呈した高齢発症の Alexander 病

愛知医科大学加齢医科学研究所　神経病理学　吉田眞理、橋詰良夫
国立東名古屋病院　神経内科　饗場郁子
名古屋医療センター　神経内科　奥田聡
京都府立医科大学大学院　神経病態制御学　中川正法

症例は死亡時 73 歳女性.（既往歴）29 歳時に両側の網膜剥離により光覚弁となる.（家族歴）弟は 58 歳時行動異常で発症し進行性核上性麻痺（progressive supranuclear palsy: PSP）と診断され 68 歳時死亡．長男は歩行障害があり 45 歳時自殺.（現病歴）62 歳時より幻覚、幻聴、64 歳時より歩行障害が出現、65 歳時 PSP を疑われた．MRI では初期から著明な脳幹、特に延髄の萎縮と前頭側頭葉の萎縮を認めた．徐々に無動無言状態となり、末期にＳ状結腸癌を合併し死亡、全経過 11 年.（神経病理学的所見）(1) 肉眼的には未固定脳重 800g、割面では大脳皮質・白質の萎縮軟化が強く、延髄は高度萎縮を示した．(2) 組織学的には大脳白質の有髄線維の脱落と粗鬆化が強く、oligodendroglia は残存しているが astrocyte の増生が乏しかった．黒質の細胞脱落を認め、延髄は中脳、橋に比してきわめて小さく、錐体では小径有髄線維の脱落が強く、脊髄錐体路の変性を認めた．脳室上衣下や、黒質、延髄網様体、錐体路、脊髄前角の血管周囲には Rosenthal fibers(RFs)を多数認めた．(3) 視神経萎縮 (4) NFT Braak stageII、老人斑や Lewy 小体は認めなかった.（遺伝子診断）GFAP exon 4 の Arg258Cys の変異を認めた.（考察）A 病は小児期に発症し RFs が出現し leukodystrophy をきたす疾患として知られているが、近年 GFAP 遺伝子異常が明らかになり，成人発症例も報告されている．成人発症例の臨床特徴は，進行性の痙性麻痺，球麻痺/仮性球麻痺，口蓋ミオクローヌスであり，MRI では著明な延髄および上部脊髄の萎縮が特徴とされている．通常，大脳白質異常は軽度か目立たないとされているが，本例では著明な白質変性をきたし，初期から前頭側頭型認知症が前景となった点が特徴である．高齢者の白質変性の鑑別疾患として A 病は重要である．

演題４

GFAP 遺伝子の missense 変異(R276L)を有する成人型 Alexander 病の新たな 2 症例

自治医科大学　神経内科　滑川道人、嶋崎晴雄、本多純子、中野今治
山梨大学医学部　血液内科　迫江公己
同　神経内科　瀧山嘉久

＜背景＞　2002 年に我々が報告した，病理学的に確定された遺伝性成人型 Alexander 病における GFAP 遺伝子の missense 変異(c.827G>T, p.R276L)は，現在まで同じ変異の報告がない．GFAP 遺伝子内には SNPs も少なくなく，missense 変異が疾患責任変異であることを確定するには慎重を要する．
＜目的＞　この変異を持つ，新たな Alexander 病の症例を探索する．
＜方法＞　本症に特徴的な延髄～頸髄の著明な萎縮(tadpole appearance)を呈する 7 例で GFAP 遺伝子検査を施行した．
＜結果＞　2 例（いずれも孤発例）で上記変異を認め，4 例では別の GFAP 遺伝子変異を同定した．1 例では変異がなかった．なおこの 2 例では，それ以外の exon および exon-intron junction 領域に（SNPs を含め）異常はなく，さらに 88 例（正常対照 78 例，疾患対照 10 例）では，この変異は認めなかった．
＜症例呈示＞　患者 1：60 歳男性．46 歳時の脳挫傷を契機に，性格変化（易怒性）．50 歳頃より呂律緩慢，57 歳時に歩行障害が出現．緩徐進行．痙性四肢不全麻痺，仮性球麻痺，失調，眼振，および認知機能障害を認めた．頭部 MRI では典型的な tadpole appearance とともに，両側基底核に T2 高信号域あり．患者 2：23 歳女性．6 歳頃から周期性嘔吐が出現し，発育遅延．11 歳時精査入院．頭部 MRI にて，延髄背側に 7mm 大の造影病変あり．2 年後，造影効果は消褪し，同時期から周期性嘔吐も消失．現在でも神経学的には正常だが，経時的な頭部 MRI では延髄～頸髄萎縮が進行している．
＜考察＞　症例 1 からは，外傷を契機に ALX が発症する可能性が示唆され，また成人型 ALX でも基底核病変がありうることが判明した．症例 2 からは，「発作性・周期性嘔吐」は若年発症 ALX の症状であること，症状が停止・自然寛解することがあることが確認され，さらに tadpole appearance の形成過程が観察できた．なお今回の 2 症例と以前の 1 家系とは血族関係はないが，同一地方出身者であり，創始者効果の存在も疑われる．
＜結論＞　GFAP 遺伝子 missense 変異（c.827G>T, p.R276L)が，疾患責任変異である更なる臨床的証拠を呈示した．

演題5

家族性Alexander病(V87G)2剖検例の臨床・病理

鹿児島大学医歯学総合研究科	神経内科・老年病学	岡本裕嗣、児玉大介、高嶋　博
岩尾病院		中村尚人
鹿児島大学	分子病理病態研	出雲周二
京都府立医大	神経内科	中川正法

A. 研究目的　孤発例の報告が多いAlexander病において、1家系2剖検例を中心に臨床・病理学的に検討した. Rosenthal fibers (RFs)の本症における役割は未解決のままである. 同一遺伝子変異を有し異なる表現型を示す本家系における RFs の出現具合などについて検討した. また本疾患発症のメカニズムについて明らかにするためにグルタミン酸トランスポーターに対する免疫染色を行い検討した.

B. 研究方法　*GFAP*遺伝子V87G点変異を有す家系内に発症した若年型、 成人型の2剖検例を中心に臨床症状, MRI, 病理所見について比較した. 免疫染色ではアストロサイトに発現するとされるEAAT-2に対する抗体などを用いて検討した.

C. 研究結果　症例1は66歳女性. 発症時53歳で, 小脳症状, 錐体路症状と口蓋ミオクローヌスを伴う嚥下障害を認め, MRI で軽度の白質病変と共に著明な延髄・脊髄の萎縮を認めた. 症例2は40歳男性. 幼少時発症で精神発達遅滞を認め, 30歳時異常行動出現, 運動失調と錐体路症状を認め, MRI でびまん性の白質病変を認めた. 剖検例では共に RFs を認めたが, 画像・臨床上は重症に見える若年型の症例2では目立たなかった. またGFAP染色では異形のアストロサイトがびまん性に認められた. EAAT-2染色では症例1, 2共にびまん性の低下がみられた.

D. 考察　RFs は必ずしも神経細胞障害の主たる原因ではなく, アストロサイトの機能障害に伴う蓄積物である可能性がある. EAAT-2 の染色性の低下は構造的に異常が少ない部位でも確認でき, アストロサイトの機能異常が病初期から存在することが考えられた. EAAT-2 はグルタミン酸代謝に重要な役割を有すトランスポーターである. 本症の発症にグルタミン酸代謝異常が関与している可能性が疑われた. 今後アストロサイト病としての機能解析をさらに検討することが重要であると考えられた.

演題 6

変異 GFAP 導入による Alexander 病ショウジョウバエモデル作成の試み

京都府立医科大学大学院　神経内科　笹山博司、中川正法
京都工芸繊維大学大学院　染色体工学　山口政光、永井里佳

【目的】　現在までに、Alexander 病のモデルとして培養細胞、マウスを使った研究が行われてきたが、うまくいっていない．そこでショウジョウバエのモデルを作製し研究を行う．
【方法】　遺伝子導入をさせるための GFAP 遺伝子発現ベクターを作製した．この発現ベクターは W 遺伝子をマーカーとして持つがヒト GFP 遺伝子も同時に導入した．作製したベクターをショウジョウバエの受精卵にマイクロインジェクションを行い遺伝子導入させた．GFAP 遺伝子を保有するショウジョウバエは表現型で赤眼になるので、赤眼のショウジョウバエを回収した．赤眼のショウジョウバエとバランサー染色体を持つショウジョウバエとを交配させた．
【結果】　変異 GFAP 遺伝子を導入したショウジョウバエに赤眼が見られた．その赤眼を 1 匹ずつ回収し、バランサー染色体を持つショウジョウバエ系統と交配し、次世代で産まれてくるショウジョウバエで line 化を行う．
【考察】　ショウジョウバエとヒトは生物としての基本的仕組みにそれほど違いがない．ショウジョウバエは遺伝子の効果が表現型として現れるので、ヒトの遺伝病の病気の原因を明らかにする上でも大変有用である．本研究で、モデルショウジョウバエを用いて、Alexander 病の原因究明が可能となる．

研究成果の刊行物・別冊

Neuroscience Letters 458 (2009) 11–14

Contents lists available at ScienceDirect

Neuroscience Letters

journal homepage: www.elsevier.com/locate/neulet

The process of inducing GFAP aggregates in astrocytoma-derived cells is different between R239C and R416W mutant GFAP. A time-lapse recording study

Tomokatsu Yoshida*, Hiroshi Sasayama, Masanori Nakagawa

Department of Neurology, Graduate School of Medical Science, Kyoto Prefectural University of Medicine, Kawaramachi Hirokoji, Kajii-chou 465, Kamigyo-ku, Kyoto 602-0841, Japan

ARTICLE INFO

Article history:
Received 19 December 2008
Received in revised form 20 February 2009
Accepted 8 April 2009

Keywords:
Alexander disease
Glial fibrillary acidic protein
Astrocytes
Time-lapse recording

ABSTRACT

Alexander disease (ALX) is a rare neurodegenerative disease caused by the gene mutations encoding glial fibrillary acidic protein (GFAP). The formation of aggregates in the cytoplasm of astrocytes, which mainly consists of GFAP, is characteristic of ALX. To examine the dynamic process of aggregates between the different domains of GFAP, we performed time-lapse recording on two different mutant GFAP. R239C and R416W *GFAP* mutations located in the rod domain and tail domain, respectively, were transfected into astrocytoma-derived cells, and their real-time dynamics were observed using time-lapse recording. Our time-lapse recording study indicated that the process of inducing aggregates would be different between R239C and R416W. In GFP-R239C cells, 32.4% first appeared as aggregates, and clusters of aggregates in the cytoplasm tended to move inward and form amorphous aggregates. On the other hand, 82.0% of GFP-R416W cells first showed disrupted GFAP, with a bubble-like or ring-like structure; however, most cells maintained their structure and were capable of cell division. Our result indicates that the mechanism of GFAP aggregation depends on the domain in which the point mutation is located. A different approach to ALX therapy should be considered according to the domain of GFAP.

Alexander disease (ALX) is a rare neurodegenerative disorder characterized by white matter degeneration, and the formation of cytoplasmic inclusions called Rosenthal fibers can be demonstrated in astrocytes in pathological studies [1]. Rosenthal fibers, which accumulate particularly in astrocyte end-feet in the subpial and perivascular zones, consist of glial fibrillary acidic protein (GFAP), heat shock protein 27 (HSP27) and αB-crystallin [7,17,6]. Clinically, ALX is classified into three subtypes: infantile, juvenile and adult forms based on the age at disease onset. The infantile form is the most common and severe and usually presents between birth and 2 years of age with developmental delay, megalocephaly, spasticity, and seizures. The adult form is milder and presents with spastic paresis and ataxia, with or without palatal myoclonus. Genetically, heterozygous *GFAP* mutations have been found in patients with ALX [2]. The corresponding domain is composed of the head domain, alpha-helical rod domain and tail domain. Most GFAP mutations are located in the rod domain and few in the tail and head domains [9], although the genotype–phenotype correlation is unknown; V87G mutation can clinically vary even between affected members of the same family who carry exactly the same mutation [13]. R416W mutation has been found in all three forms of ALX [2,9,12].

ALX is considered a disorder of astrocytes associated with protein misfolding and aggregation because GFAP transgenic mice overexpressing human wild-type GFAP showed characteristic pathological changes and clinical features [10]. The mechanisms leading to aggregate formation, which were considered models of Rosenthal fibers, were investigated in recent studies. Mutant GFAP decreases the solubility of normal GFAP and alters the organization of the GFAP network [5]. Insufficient amounts of plectin, an intermediate filament-associated protein, promote GFAP aggregation and Rosenthal fiber formation [16]. GFAP aggregates stimulate autophagic pathways, regulated by p38/MAPK and mTOR signaling pathways [15]. Our previous study using a migration assay suggested that functional abnormalities of astrocytes might be induced prior to GFAP aggregation and that this functional alteration depends on the domain in which the point mutation is located [18].

In this study, to examine the dynamic process of aggregation between different domains of GFAP, we performed time-lapse recording of R239C and R416W mutant GFAP, located in the rod and tail domains, respectively.

The coding region of human genomic DNA was amplified by polymerase chain reaction (PCR) using the following primers with

* Corresponding author. Tel.: +81 75 251 5793; fax: +81 75 211 8645.
E-mail address: toyoshid@koto.kpu-m.ac.jp (T. Yoshida).

0304-3940/$ – see front matter © 2009 Elsevier Ireland Ltd. All rights reserved.
doi:10.1016/j.neulet.2009.04.032

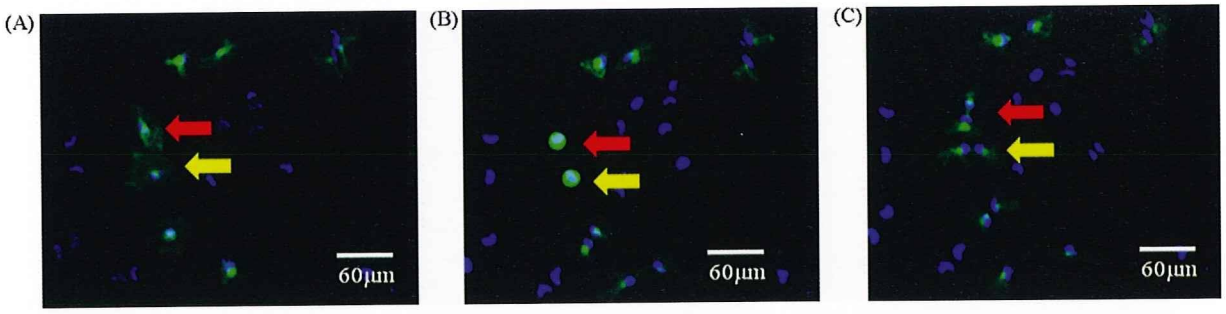

Fig. 1. Time-lapse recording of GFP-wild-type GFAP cells at 10× magnification. Cells shown with red and yellow arrows demonstrated filamentous distribution of GFAP and cell division.

restriction sites—sense: GFAP-F.EcoRI 5′-CGGGAATTCAGCAGGATG-GAGAGGAGACG-3′, antisense: GFAP-R.Bam 5′-GGCGGATCCCAGA-GGCCACCAGGTGGGTC-3′. After purification, PCR products were digested with EcoRI and BamHI and ligated into EcoRI and BamHI sites of pUC18 plasmid (Takara Shuzo, Otsu, Japan). Point mutations, R239C (*GFAP* C729T) and R416W (*GFAP* C1260T), were generated as described for the LA PCR in vitro mutagenesis kit (Takara Shuzo, Otsu, Japan). Following digestion with EcoRI and SphI, each of the mutated DNA fragments was ligated into the EcoRI and SphI sites of pUC18. The constructs were sequenced using an ABI PRISM 310 autosequencer (PE Applied Biosystems, Foster City, CA, USA). To prepare *GFAP* tagged with a GFP vector (GFP-R239C and GFP-R416W), each of the pUC18 plasmids containing mutant *GFAP* was amplified by PCR using the following primers with restriction sites—sense: GFAP-F/Hind-GFP 5′-CGAAGCTTGATTACGAATTCAGCAGG-3′, antisense: GFAP-R/pAcGFP-Bam 5′-GAGGATCCGTCCTGCCTCACATCACA-3′. After purification, the PCR products were digested with HindIII and BamHI and ligated into the HindIII and BamHI sites of pAcGFP-C3 (Becton Dickinson, Franklin Lakes, NJ, USA).

Human astrocytoma-derived cells (U251) were grown in RPMI 1640 medium (Nikken Biochemical Laboratory, Kyoto, Japan) supplemented with 10% fetal bovine serum (FBS) and amphotericin B (0.125 μg/ml). One day before transfection, 4×10^4 cells were plated onto a 35-mm plate (Becton Dickinson, Franklin Lakes, NJ, USA). Cells on each plate were transfected for 2 h using 2.0 μg plasmid with transfection reagent (Lipofectamin 2000®, Invitrogen, Japan). After transfection, cells were washed with medium containing 10% FBS to terminate the reaction. Cells were assayed for the expression of the transfected gene after 48 h. Just before the time-lapse recording, cell nuclei were stained with Hoechst 33342 at 37 °C for 30 min. A plate for real-time acquisition was placed in the incubator at 37 °C with 5% CO_2/95% air on the stage of a fluorescence microscope (BIOREVO BZ-9000, KEYENCE). Time-lapse images were acquired every 20 min for 24 h at 10 or 40× magnification.

Real-time images of both GFP-wild-type GFAP (GFP-Wt) and GFP-mutant GFAP showed two initial phenotype patterns: an apparently normal filamentous network, or aggregates. Overall, 86.1% of GFP-Wt cells ($n = 79$) first appeared with a normal filamentous network and 95.6% ($n = 65$) maintained the filamentous network and were capable of cell division (Fig. 1). The remaining 13.9% of GFP-Wt cells ($n = 11$) first appeared as aggregates. Almost all of these cells (90.9%, $n = 11$) were unchanged and were incapable of cell division. In GFP-R239C cells ($n = 293$), 32.4% ($n = 95$) first appeared as aggregates. In such cells, a cluster of aggregates in the cytoplasm tended to move inward and form amorphous aggregates (Fig. 2). These aggregates were incapable of cell division. Overall, 82.0% of GFP-R416W cells ($n = 73$) first appeared as a filament network at 10× magnification; however, these cells showed that the filaments were constructed of a bubble-like or ring-like structure at 40× magnification (Fig. 3); 79.5% of such cells ($n = 58$) maintained their structure and were capable of cell division, whereas 20.5% of cells that appeared with an apparently filamentous network ($n = 15$) were induced to aggregate.

Our time-lapse recording study indicated that the process of inducing aggregates would be different between R239C and R416W. R239 is located in the helical rod domain or central helical domain in *GFAP*, which is considered important for interfilament network formation, filament assembly and stabilization of subunits [11]. A previous time-lapse recording study by Mignot et al. showed that aggregates of R236H, which was also located in the rod domain of *GFAP*, either disappeared, associated with cell survival, or coalesced in a huge juxtanuclear structure associated with cell death [4]. Therefore, mutant GFAP in the rod domain, including R239C, might be unable to maintain the fundamental filamentous architecture of GFAP and be induced to aggregate, suggesting that the degree of severity of mutant GFAP in the rod domain depends on the degree of disruption of the fundamental structure, which may have a dominant effect on wild-type GFAP.

R416 is located in the tail domain, which is conserved between all type III intermediate filament proteins and is thought to play a role in stabilizing protofibrillar interactions and filament diameter [3]. Furthermore, R416W GFAP is expected to alter interactions with other cytoskeletal elements [11]. Perng et al. reported that molecu-

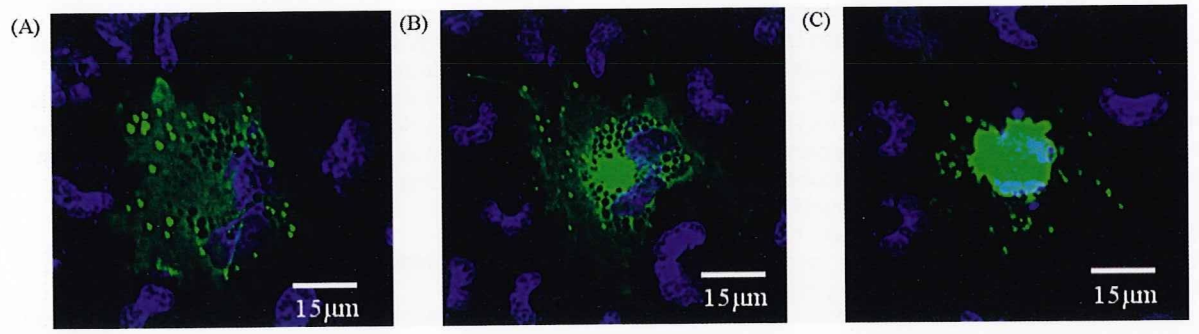

Fig. 2. Time-lapse recording of a GFP-R239C cell. About 30% of these cells first showed a cluster of aggregates in the cytoplasm (A) and tended to move inward (B), and finally formed amorphous aggregates (C). This type of aggregate was incapable of cell division.

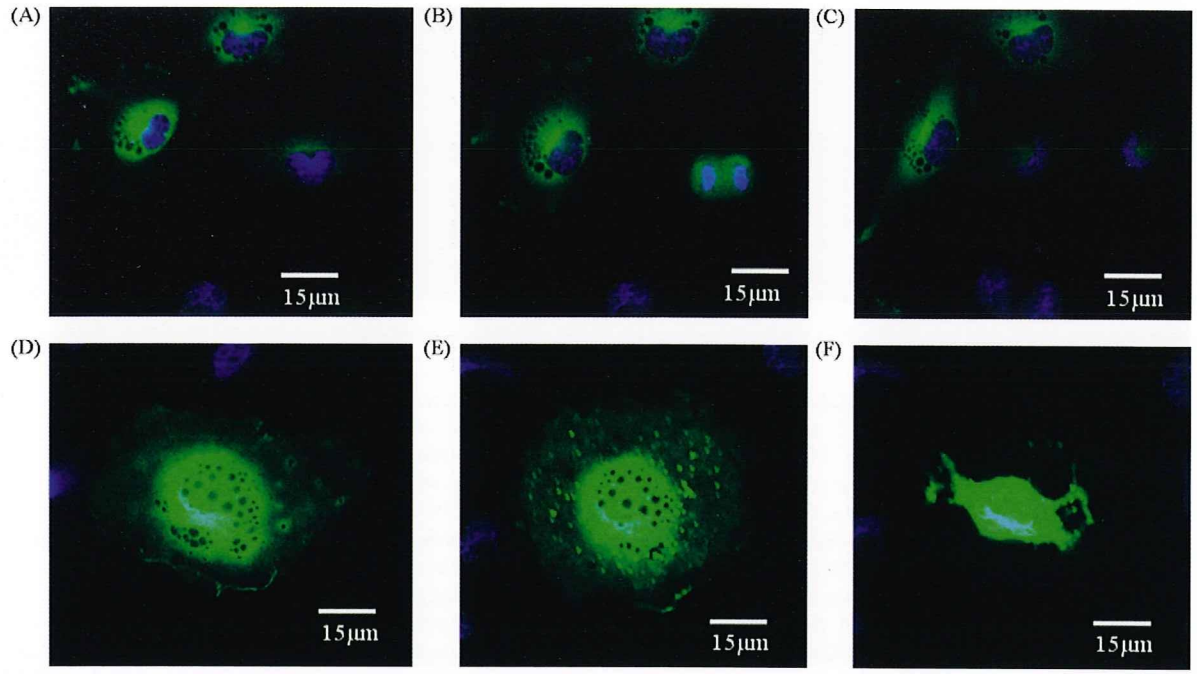

Fig. 3. Time-lapse recording of a GFP-R416W cell. These cells showed filaments constructed of a bubble-like or ring-like structure at high magnification (A and D). 79.5% of such cells maintained the structure and were capable of cell division (B and C). In the other cells, clusters of small aggregates emerged from the cytoplasm (E) and formed large aggregates (F). This type of aggregate was incapable of cell division.

Table 1
Dynamics of astrocytoma cells transfected with wild-*GFAP* and mutant *GFAP* in time-lapse experiment.

GFP-Wt		
Initial phenotype	filamentous network 86.1%(n=68/79)	aggregates 13.9%(n=11/79)
Dynamic evolution	network 95.6%(n=65) / aggregates 4.4%(n=3)	network 9.1%(n=1) / aggregates 90.9%(n=10)
GFP-R239C		
Initial phenotype	filamentous network 67.6%(n=198/293)	aggregates 32.4%(n=95/293)
Dynamic evolution	network 94.4%(n=187) / aggregates 5.6%(n=11)	network 9.5%(n=9) / aggregates 90.5%(n=86)
GFP-R416W		
Initial phenotype	filamentous network 82.0%(n=73/89)	aggregates 18.0%(n=16/89)
Dynamic evolution	network 79.5%(n=58) / aggregates 20.5%(n=15)	network 6.3%(n=1) / aggregates 93.7%(n=15)

lar chaperones, including HSP27 and αB-crystallin, were associated with the formation of GFAP aggregates and led to astrocyte malfunction [14]. In our study, many cells with R416W GFAP were able to undergo cell division, although the filamentous structure of these cells was apparently disrupted. Our results suggested that these cells could maintain the fundamental structure of GFAP, and that the alteration of R416W GFAP function in astrocytes depended on other elements which interact with GFAP, supporting the fact that the phenotype of mutant *GFAP* in the tail domain shows a variety of clinical features of ALX with varying severity [2,9,8].

A small population of cells with aggregates recovers filamentous network morphology during time-lapse recording (Table 1). Some of these cells were not pathological aggregates but apparent aggregates in cell division, because these cells divided and converted to filamentous network morphology in the early stage during recording; however, the rest converted to filamentous network morphology without cell division, suggesting that this kind of aggregate may disappear spontaneously, independent of cell division.

In summary, our real-time imaging study using time-lapse recording indicates that the mechanism of GFAP aggregation depends on the domain in which the point mutation is located and may be able to explain the difference in clinical features between the domains. A different approach to ALX therapy should be considered according to the domain of GFAP.

Acknowledgments

This work was supported by Alexander disease research grants from the Intractable Disease Research Grants, from the Ministry of Health, Labour, and Welfare of the government of Japan.

References

[1] W.S. Alexander, Progressive fibrinoid degeneration of fibrillary astrocytes associated with mental retardation in a hydrocephalic infant, Brain 72 (1949) 373–381.

[2] M. Brenner, A.B. Johnson, O. Boespflug-Tanguy, et al., Mutations in *GFAP*, encoding glial fibrillary acidic protein, are associated with Alexander disease, Nat. Genet. 27 (2001) 277–286.

[3] E. Fuchs, The cytoskeleton and disease: genetic disorders of intermediate filaments, Ann. Rev. Genet. 30 (1996) 197–231.

[4] P.A. Hall, D.A. Levison, A.L. Woods, et al., Proliferating cell nuclear antigen (PCNA) immunolocalization in paraffin sections: an index of cell proliferation with evidence of deregulated expression in some neoplasms, J. Pathol. 162 (1990) 285–294.

[5] V.C. Hsiao, R. Tiao, H. Long, et al., Alexander disease mutation of *GFAP* causes filament disorganization and decreased solubility of GFAP, J. Cell Sci. 118 (2005) 2057–2065.

[6] T. Iwaki, A. Kume-Iwaki, R.K. Liem, J.E. Goldman, Alpha-B-crystallin is expressed in non-lenticular tissues and accumulates in Alexander's disease brain, Cell 57 (1989) 71–78.

[7] A.B. Johnson, A. Bettica, On-grid immunogold labeling of glial intermediate filaments in epoxy-embedded tissue, Am. J. Anat. 185 (1989) 335–341.

[8] T. Kinoshita, T. Imaizumi, Y. Miura, et al., A case of adult-onset Alexander disease with Arg416Trp human glial fibrillary acidic protein gene mutation, Neurosci. Lett. 350 (2003) 169–172.

[9] R. Li, A.B. Johnson, G. Salomons, et al., Glial fibrillary acidic protein mutations in infantile, juvenile, and adult forms of Alexander disease, Ann. Neurol. 57 (2005) 310–326.

[10] A. Messing, W.H. Mark, K. Galles, et al., Fatal encephalopathy with astrocyte inclusions in GFAP transgenic mice, Am. J. Pathol. 152 (1998) 391–398.

[11] C. Mignot, C. Delarasse, S. Escaich, B.D. Gaspera, E. Noé, et al., Dynamics of mutated GFAP aggregates revealed by real-time imaging of an astrocyte model of Alexander disease, Exp. Cell Res. 313 (2007) 2766–2779.

[12] Y. Nobuhara, K. Nakahara, I. Higuchi, et al., Juvenile form of Alexander disease with *GFAP* mutation and mitochondrial abnormality, Neurology 63 (2004) 1302–1304.

[13] Y. Okamoto, H. Mitsuyama, M. Jonosono, et al., Autosomal dominant palatal myoclonus and spinal cord atrophy, J. Neurol. Sci. 19 (2002) 71–76.

[14] M.D. Perng, M. Su, S.F. Wen, et al., The ALX-causing glial fibrillary acidic protein mutant, R416W, accumulates into Rosenthal fibers by a pathway that involves filament aggregation and the association of αB-crystallin and HSP27, Am. J. Hum. Genet. 79 (2006) 197–213.

[15] G. Tang, Z. Yue, Z. Talloczy, T. Hagemann, W. Cho, A. Messing, D.L. Sulzer, J.E. Goldman, Autophagy induced by Alexander disease-mutant GFAP accumulation is regulated by p38/MAPK and mTOR signaling pathways, Hum. Mol. Genet. 17 (2008) 1540–1555.

[16] R. Tian, M. Gregor, G. Wiche, J.E. Goldman, Plectin regulates the organization of glial fibrillary acidic protein in Alexander disease, Am. J. Pathol. 168 (2006) 888–897.

[17] N. Tomokane, T. Iwaki, J. Tateishi, et al., Rosenthal fibers share epitopes with alpha-B-crystallin, glial fibrillary acidic protein, and ubiquitin, but not with vimentin: immunoelectron microscopy with colloidal gold, Am. J. Pathol. 138 (1991) 875–885.

[18] T. Yoshida, Y. Tomozawa, T. Arisato, Y. Okamoto, H. Hirano, M. Nakagawa, The functional alteration of mutant GFAP depends on the location of the domain: morphological and functional studies using astrocytoma-derived cells, J. Hum. Genet. 52 (2007) 362–369.

Movement Disorders
Vol. 24, No. 9, 2009, pp. 1393–1406

Letters to the Editor Related to New Topics

Novel *GFAP* Mutation in Patient with Adult-Onset Alexander Disease Presenting with Spastic Ataxia

Adult-onset Alexander disease is rare and clinically characterized by slowly progressive signs of brainstem and spinal cord involvement.[1] Missense mutations in the gene encoding the glial fibrillary acidic protein (*GFAP*) have been identified as a genetic basis for Alexander disease.[2] We here report a Japanese patient with adult-onset Alexander disease with a novel *GFAP* mutation.

A 36-year-old man of Japanese descent, a child of nonconsanguineous parents, with a 10-year history of slowly progressive gait disturbance, was referred to us. His early motor and intellectual development were normal. Neurological examination revealed rhythmic ocular nystagmoid movement, dysarthria, truncal and limb ataxia, increased muscle stretch reflex with bilateral Babinski sign, and spasticity in his lower extremities. Palatal myoclonus was not noted. He was ambulatory, but his gait was unsteady owing to ataxia and spasticity in the lower extremities.

Brain MRI demonstrated a marked atrophy of the medulla oblongata and cervical spinal cord, and a mild atrophy of the cerebellar hemisphere (Fig. 1A). Fluid attenuation inversion recovery (FLAIR) images revealed abnormal hyperintensities in cerebellar dentate nucleus (Fig. 1B) and the periventricular white matter (Fig. 1C).

Molecular genetic analysis of *GFAP* was performed using the patient's genomic DNA after obtaining written informed consent. Sequence analysis revealed a heterozygous 302T > C substitution in exon 1 of *GFAP*, leading to an L101P substitution. The L101P substitution is located in the C-terminal end of the 1A rod domain of *GFAP* occurring in a highly conserved amino acid residue across species (Fig. 1D). The sequence change was confirmed by restriction fragment length polymorphism (RFLP) using enzyme digestion by *Bcg*I in the patient and 100 normal control subjects (Fig. 1E).

To obtain biochemical evidence of pathogenecity of the novel *GFAP* L101P mutant, we transfected wild-type and mutant GFAP, and examined the solubility of the GFAP protein. Samples were sequentially extracted with different stringent buffers and subjected to western blot analysis (see Supplementary methods). The well-characterized mutant R416W GFAP was largely recovered from the detergent-resistant S2 fraction because of the decreased solubility of mutant GFAP (Fig. 1F, lane 8) as previously reported.[3,4] In this assay, wild-type GFAP was predominantly detected in the soluble S1 fraction (Fig. 1F, lane 2). In contrast, the mutant L101P GFAP was largely observed in the detergent-resistant S2 fraction (Fig. 1F, lane 7). Transfected cells were further analyzed for GFAP assembly by confocal microscopy (see Supplementary methods). Whereas wild-type GFAP displayed cytoplasmic distribution with a filamentous network, the L101P mutant yielded an irregular dot-like structure largely lacking the filamentous structure (Supp. Info. Fig.).

In this study, we identified a novel *GFAP* mutation in a Japanese patient with adult-onset Alexander disease presenting with slowly progressive spastic ataxia. The parents of the patient are unaffected; hence, the mutation seems to arise *de novo* in the patient as in most cases of Alexander disease.[1] Indeed, the mother did not carry the mutation. Unfortunately, DNA sample was unavailable from the father, who has recently died of heart disease.

GFAP is a member of the intermediate filament family with a conserved central helical rod domain flanked by the head and tail domains (Fig. 1D). The L101P mutation detected in the patient is located in the coil 1A rod domain, which is considered to play an essential role in filament formation. Mutations of the α-helix regions in the rod domain are considered to alter the charge and hydrophobic interactions within coiled coils.[4] Thus, mutations in the domain may affect the solubility of GFAP, which is supported by our biochemical experiments using cells expressing mutant GFAP.

To date, more than 10 GFAP missense mutations associated with adult-onset Alexander disease have been found, with nearly all occurring in the rod domain.[1,5–7] The genotype–phenotype correlation in Alexander disease has been poorly understood particularly in adult-onset cases, probably owing to the very small number of patients. Alexander disease in our patient is clinically characterized by slowly progressive spastic ataxia with bulbar signs without palatal myoclonus. In patients with adult-onset Alexander disease, bulbar symptoms, gait ataxia, and spasticity are common clinical features, whereas ocular motor abnormalities, autonomic dysfunctions, and palatal myoclonus have been reported with varying frequency.[1,5–7]

Our patient exhibited atrophy of the medulla and spinal cord, and abnormal hyperintensities of the periventricular white matter and cerebellar dentate nucleus on FLAIR images. The characteristic atrophy of the medulla and spinal cord is invariably present in adult-onset Alexander disease.[5–7] In contrast, leukoencephalopathy and abnormal signal intensities of the cerebellum are not always observed in adult-onset cases.[5–7] The question of why missense mutations in the same critical domain of GFAP result in such different clinical phenotypes and MRI findings in Alexander disease is intriguing and deserves further attention and elucidation.

Acknowledgments: This study was supported in part by Grant-in-Aid (18590930) for scientific research from the MEXT, Japan and a grant from the Research Committee for Ataxic Diseases, the Ministry of Health, Labor and Welfare, Japan.

Additional Supporting Information may be found in the online version of this article.

Hiroyuki Kaneko and Masaki Hirose contributed equally to this study

Potential conflict of interest: Nothing to report.

Published online 1 May 2009 in Wiley InterScience (www.interscience.wiley.com). DOI: 10.1002/mds.22556

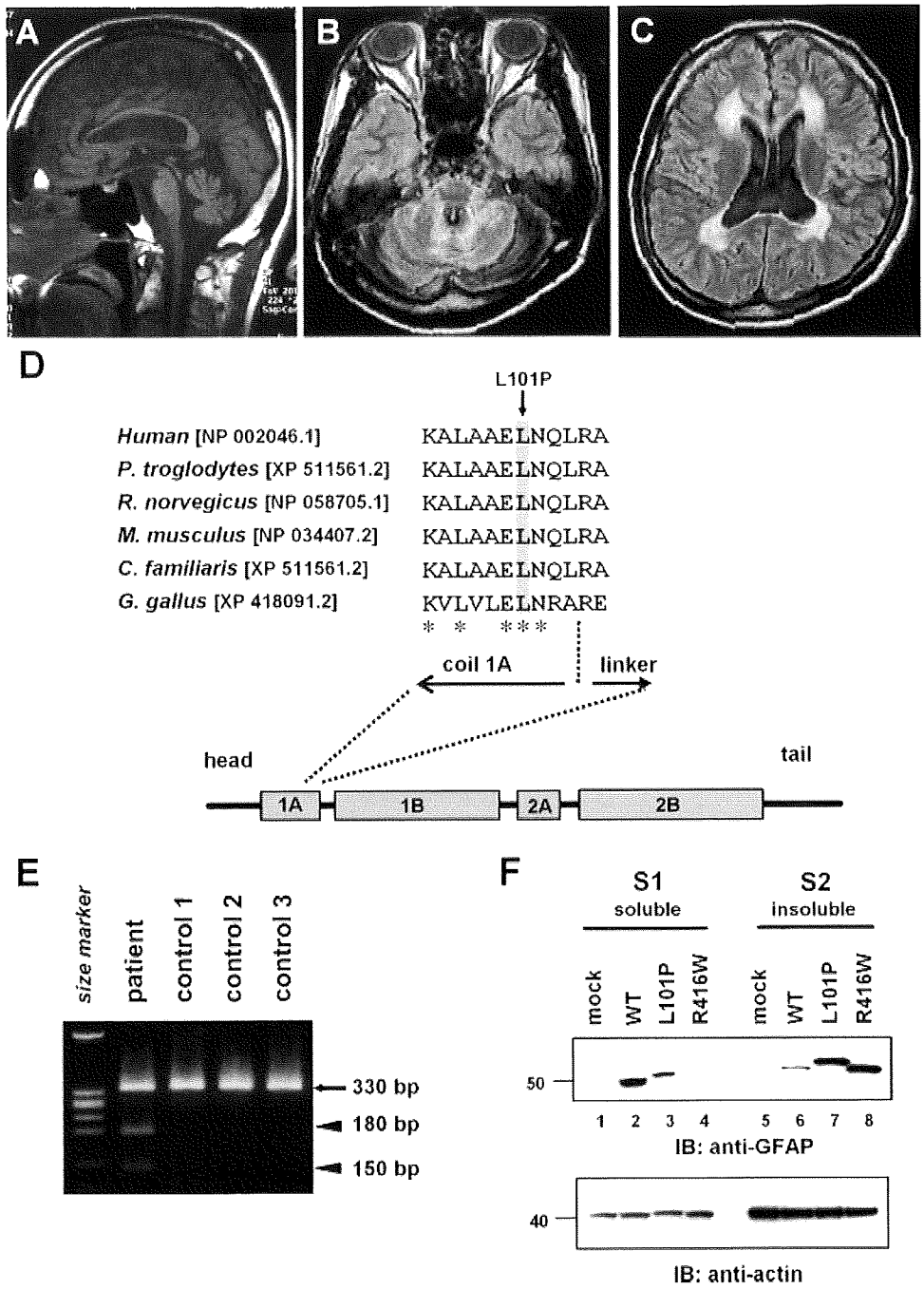

FIG. 1. Brain MRI of patient. (**A**) A midsagittal T1-weighted image shows atrophy of the medulla oblongata and the cervical spinal cord. (**B**) An axial FLAIR scan shows signal abnormality of the cerebellum. (**C**) White matter hyperintensity in the frontal and occipital portions is observed in a FLAIR image. (**D**) Localization of novel L101P mutation. Schematic of GFAP is shown. Boxes indicate the four α-helical subdomains within the central rod domain, separated by nonhelical linkers. Amino acid sequences of GFAP among species were compared by multiple sequence alignments using the Clustalw algorithm. The conserved amino acids are indicated by asterisks. (**E**) The mutation is confirmed by RFLP analysis. The 330-bp wild-type PCR product (arrow) was not digested with *Bcg*I and generated a single fragment. The mutation resulted in the cleavage of the product into 180 and 150 bp (arrowhead). (**F**) Solubility of GFAP in culture cells. C6 cells were transiently transfected with the expression vector encoding wild-type or mutant (L101P or R416W) GFAP. Transfected human GFAP (~50 kDa) was detected with the monoclonal anti-human GFAP antibody, which does not react with endogenous rat GFAP (upper panel, lanes 1 and 5). L101P GFAP (lanes 3 and 7) migrates slightly slower than the wild-type or R416W GFAP. The same samples were blotted with the anti-actin antibody to show that comparable amounts of proteins were loaded (lower panel).

Hiroyuki Kaneko, MMed
Department of Neurology
Brain Research Institute
Niigata University
Niigata, Japan
Department of Molecular Neuroscience
Brain Research Institute
Niigata University
Niigata, Japan

Masaki Hirose, MD
Department of Neurology
Brain Research Institute
Niigata University
Niigata, Japan

Shinichi Katada, MD
Department of Neurology
Brain Research Institute
Niigata University
Niigata, Japan
Department of Molecular Neuroscience
Brain Research Institute
Niigata University
Niigata, Japan

Toshiaki Takahashi, MD
School of Health Science, Faculty of Medicine
Niigata University
Niigata, Japan

Satoshi Naruse, MD
Department of Neurology
Brain Research Institute
Niigata University
Niigata, Japan

Miyuki Tsuchiya, BS
Department of Molecular Neuroscience
Brain Research Institute
Niigata University
Niigata, Japan

Tomokatsu Yoshida, MD
Masanori Nakagawa, MD
Department of Neurology
Graduate School of Medical Science
Kyoto Prefectural University of Medicine
Kyoto, Japan

Osamu Onodera, MD
Department of Molecular Neuroscience
Brain Research Institute
Niigata University
Niigata, Japan

Masatoyo Nishizawa, MD
Department of Neurology
Brain Research Institute
Niigata University
Niigata, Japan

Takeshi Ikeuchi, MD*
Department of Molecular Neuroscience
Brain Research Institute
Niigata University
Niigata, Japan
**E-mail: ikeuchi@bri.niigata-u.ac.jp*

References

1. Li R, Johnson AB, Salomons G, et al. Glial fibrillary acidic protein mutations in infantile, juvenile, and adult forms of Alexander disease. Ann Neurol 2005:57;310–326.
2. Brenner M, Johnson AB, Boespflug-Tanguy O, Rodrigues D, Goldman JE, Messing A. Mutations in GFAP, encoding glial fibrillary acidic protein, are associated with Alexander disease. Nat Genet 2001;27:117–120.
3. Yoshida T, Tomozawa Y, Arisato T, Okamoto Y, Hirano H, Nakagawa M. The functional alteration of mutant GFAP depends on the location of the domain: morphological and functional studies using astrocytoma-derived cells. J Hum Genet 2007;52:362–369.
4. Perng MD, Su M, Wen SF, et al. The Alexander disease-causing glial fibrillary acidic protein mutant, R416W, accumulates into Rosenthal fibers by a pathway that involves filament aggregation and the association of αB-crystallin and HSP27. Am J Hum Genet 2006;79:197–213.
5. Namekawa M, Takiyama Y, Aoki Y, et al. Identification of *GFAP* gene mutation in hereditary adult-onset Alexander's disease. Ann Neurol 2002;52:779–785.
6. Pareyson D, Fancellu R, Mariotti C, et al. Adult-onset Alexander disease: a series of eleven unrelated cases with review of the literature. Brain 2008;131:2321–2331.
7. Hinttala R, Karttumen V, Karttumen A, Herva R, Uusimaa J, Remes AM. Alexander disease with occipital predominance and a novel c.799G>C mutation in the GFAP gene. Acta Neuropathol 2007;114:543–545.

Early Brain Abscess: A Rare Complication of Deep Brain Stimulation

Deep brain stimulation (DBS) is successfully used for symptomatic treatment of various movement disorders. However, the technique is not without risks for adverse events related to surgery, hardware, or stimulation itself. There is a continued need for standardized reporting of adverse events related to DBS surgery, especially with respect to serious infections.[1] These include the rare complication of intracerebral infections, which if not recognized, may cause serious and long-term morbidity.

A 55-year-old man with tremor-predominant Parkinson's disease underwent unilateral DBS surgery. The electrode (3387, Medtronic, Minneapolis, MN) was placed in the right

Published online 1 May 2009 in Wiley InterScience (www.interscience.wiley.com). DOI: 10.1002/mds.22569

Acta Neuropathol (2009) 117:55–62
DOI 10.1007/s00401-008-0456-1

ORIGINAL PAPER

Increased TDP-43 protein in cerebrospinal fluid of patients with amyotrophic lateral sclerosis

Takashi Kasai · Takahiko Tokuda · Noriko Ishigami · Hiroshi Sasayama · Penelope Foulds · Douglas J. Mitchell · David M. A. Mann · David Allsop · Masanori Nakagawa

Received: 2 October 2008 / Revised: 28 October 2008 / Accepted: 28 October 2008 / Published online: 7 November 2008

Abstract There is mounting pathological, biochemical and genetic evidence that the metabolism and aggregation of the 43-kDa transactive response (TAR)-DNA-binding protein (TDP-43) play a crucial role in the pathogenesis of sporadic and some forms of familial amyotrophic lateral sclerosis (ALS). Recently, it was reported using an ELISA system that elevated levels of TDP-43 were detected in plasma samples from patients with Alzheimer's disease and frontotemporal dementia, compared to healthy controls. To determine whether quantification of TDP-43 in cerebrospinal fluid (CSF) is potentially informative in the diagnosis of ALS, we measured the concentration, by a similar ELISA method, of TDP-43 in CSF from 30 patients with ALS (diagnosed according to the revised El Escorial criteria) and 29 age-matched control patients without any neurodegenerative disease. We found that, as a group, the ALS patients had significantly higher levels of TDP-43 in their CSF than the age-matched controls (6.92 ± 3.71 ng/ml in ALS versus 5.31 ± 0.94 ng/ml in controls, $p < 0.05$), with levels of TDP-43 in CSF elevated beyond 95% upper confidence level for the control group in six (20%) of the patients with sporadic ALS. All the six patients with higher levels of CSF TDP-43 were examined within 10 months of the onset of illness. The patients examined within 10 months of onset showed significantly higher levels of CSF TDP-43 (8.24 ± 4.72 ng/ml) than those examined after 11 months or more of onset (5.41 ± 0.66 ng/ml, $p < 0.05$). These results suggest that the levels of TDP-43 in CSF may increase in the early stage of ALS. We also confirmed the existence of the TDP-43 protein in CSF from some patients with ALS, and a control subject, by western blotting of proteins immunocaptured from the CSF samples. Raised TDP-43 levels in the CSF may preempt the formation of TDP-43 pathology in the central nervous system, or correlate with early-stage TDP-43 pathology, and accordingly be a biomarker for the early stage of ALS.

Keywords Amyotrophic lateral sclerosis · TDP-43 · Cerebrospinal fluid · ELISA · Biomarker

T. Kasai · T. Tokuda (✉) · N. Ishigami · H. Sasayama · M. Nakagawa
Department of Neurology,
Kyoto Prefectural University of Medicine,
465 Kajii-cho, Kamigyo-ku, Kyoto 602-0841, Japan
e-mail: ttokuda@koto.kpu-m.ac.jp

P. Foulds · D. Allsop
Division of Biomedical and Life Sciences,
School of Health and Medicine, Lancaster University,
Lancaster LA1 4YQ, UK

D. J. Mitchell
MND Care and Research Centre,
Royal Preston Hospital, Sharoe Green Lane,
Preston PR2 9HT, UK

D. M. A. Mann
Clinical Neurosciences Research Group,
School of Translational Medicine,
Faculty of Medical and Human Sciences,
University of Manchester, Greater Manchester
Neurosciences Centre, Hope Hospital, Salford M6 8HD, UK

Introduction

Amyotrophic lateral sclerosis (ALS) is a relentlessly progressive and ultimately fatal neurodegenerative disorder characterized pathologically by the degeneration of upper and lower motor neurons and the presence of ubiquitin-positive, tau- and α-synuclein-negative cytoplasmic inclusions (UBIs) in the degenerating neurons [26, 29]. Most ALS cases are sporadic (SALS), but about 10% of ALS patients

have a positive family history (FALS), of which about 20% are caused by missense mutations in the gene for superoxide dismutase 1 (*SOD1*) [11, 25]. About 15% of ALS cases develop frontotemporal dementia (FTD)—a clinical subtype of frontotemporal lobar degeneration (FTLD) [27]—but about 50% of ALS patients will develop cognitive impairment during the course of their illness [1, 15, 27]. Recently, the 43-kDa transactive response (TAR)-DNA-binding protein (TDP-43), which is encoded by the *TARDBP* gene on chromosome 1, was identified as the major pathological protein of the motor neuron inclusions found in SALS and SOD1-negative FALS, as well as sporadic and familial FTLD with UBIs (FTLD-U) [2, 7, 8, 14, 16, 19, 28, 32]. Furthermore, missense mutations in the *TARDBP* gene in FALS and SALS have been reported, implying that abnormal TDP-43 alone may be sufficient to cause neurodegeneration [10, 13, 31, 34]. These collective studies provide evidence of a direct link between the TDP-43 protein, its aggregation, and the development of ALS. They also suggest that TDP-43 could serve as a marker candidate for SALS, for which no biological markers have yet been established to aid its clinical diagnosis. The availability of such a resource would have a major impact on clinical practice.

The TDP-43 is a 414-amino acid nuclear protein that is highly conserved across species and is ubiquitously expressed in tissues, including heart, lung, liver, spleen, kidney, muscle, and brain [4]. Previous reports suggested that physiological functions of TDP-43 might involve binding to single strand DNA, RNA, and proteins, to regulate biological processes in the nucleus [4, 17, 23]. Recently, Foulds et al. have shown that TDP-43 can be detected in human plasma by enzyme-linked immunosorbent assay (ELISA) and western blotting, and that the levels of this protein are elevated (compared to healthy controls) in some patients with Alzheimer's disease (AD) and others with FTD [9]. These findings suggest that TDP-43 is constitutively released into the extracellular space and can be detected in the body fluids, such as plasma and possibly cerebrospinal fluid (CSF). Interestingly, Foulds et al. detected elevated levels of TDP-43 protein in plasma of 22% patients with AD and 46% patients with FTD. The proportions of patients with FTD and AD showing raised plasma TDP-43 levels correspond closely to those proportions of patients known from autopsy studies to harbor TDP-43 pathological changes in their brains, and so it was concluded that raised plasma levels of TDP-43 may witness the presence of TDP-43 pathology within the brain. Pathological studies have indicated that about half of all cases with FTD have ubiquitin-positive, TDP-43-positive cytoplasmic inclusions (FTLD-U pathology) that are identical with those seen in motor neurons in ALS [15, 18, 30]. We therefore considered that the quantification of extracellular TDP-43 in plasma and CSF could offer an opportunity for the development of a molecular biomarker not only for FTLD-U, but also for ALS and related diseases. There are no previous reports that have quantified TDP-43 either in CSF or plasma samples from patients with ALS. In this study, we modified the ELISA protocol described by Foulds et al. [9] to improve its sensitivity and applied this method to measure the levels of TDP-43 in CSF from patients with ALS and control cases.

Materials and methods

CSF samples

The CSF samples were obtained from 30 patients with SALS (ages 42–85, mean ± SD 65.3 ± 10.0, see Table 1 for clinical details) and 29 age-matched control patients (ages 54–84, mean ± SD 68.8 ± 8.7). All subjects provided written informed consent to participate in the study, which was approved by the University Ethics Committee (Kyoto Prefectural University of Medicine, Kyoto, Japan). The study procedures were designed and performed in accordance with the Declaration of Helsinki. The patients with SALS examined in this study consisted of those with "definite" ($n = 17$) or "probable" ($n = 13$) ALS, diagnosed according to the revised El Escorial criteria [3]. None of the SALS patients had a family history of ALS, or SOD-1 mutations. In this study we excluded any SALS patients with dementia. The age-matched control subjects comprised neurologically normal individuals (healthy controls, $n = 13$) and controls with various neurological disorders (disease controls, $n = 16$) including patients with epilepsy ($n = 2$), cerebellar ataxia ($n = 1$), benign positional vertigo ($n = 1$), myelopathy ($n = 1$), cervical spondylosis ($n = 2$), cranial and peripheral neuropathy ($n = 6$), and myopathy ($n = 3$). None of the 29 age-matched control patients had dementia. Fresh CSF samples were collected from living SALS and control cases, and then stored at −80°C until used for the ELISA.

Immunoassay protocol

The TDP-43 in CSF was measured using a sandwich ELISA system similar to that reported by Foulds et al. [9] with small modifications. The ELISA plates (Nunc MaxiSorp, flat-bottom 96-well Black MicroWell plate, Roskilde, Denmark) were coated by overnight incubation at 4°C with 0.2 μg/ml anti-TDP-43 monoclonal antibody raised against a recombinant protein corresponding to residues 1–261 of human TDP-43 (H00023435-M01, clone 2E2-D3, Abnova Corporation, Walnut, USA), 100 μl/well, diluted in 200 mM $NaHCO_3$ buffer, pH 9.6. The plates

Table 1 Clinical details of patients with ALS at the time when CSF samples were taken and the concentration of TDP-43 in CSF

Case	Gender	Age at onset (y)	Disease duration (m)	Clinical diagnosis[a]	Bulbar sign	Dementia	CSF TDP-43 (ng/ml)
1[b]	M	74	9	Definite	–	–	19.76
2[b]	F	61	10	Definite	+	–	18.39
3[b]	M	68	4	Definite	+	–	12.05
4[b]	F	41	5	Definite	+	–	10.70
5[b]	M	74	3	Definite	+	–	8.12
6[b]	M	66	5	Probable	–	–	7.40
7	M	84	20	Definite	+	–	6.95
8	F	68	9	Definite	+	–	6.55
9	F	65	26	Definite	–	–	6.48
10	M	68	10	Probable	–	–	6.35
11	F	64	32	Definite	–	–	6.02
12	M	65	2	Probable	–	–	5.96
13	M	66	5	Probable	–	–	5.81
14	M	64	8	Probable	–	–	5.63
15	M	53	10	Probable	–	–	5.53
16	F	78	30	Probable	+	–	5.51
17	M	81	19	Probable	+	–	5.46
18	F	54	32	Probable	–	–	5.38
19	F	69	23	Definite	+	–	5.28
20	M	60	11	Probable	–	–	5.21
21	M	50	10	Definite	–	–	5.17
22	M	70	38	Probable	+	–	5.15
23	M	69	12	Definite	+	–	5.04
24	M	63	8	Definite	+	–	4.95
25	F	61	11	Definite	+	–	4.95
26	M	69	14	Probable	+	–	4.92
27	F	62	9	Definite	+	–	4.81
28	M	60	36	Probable	+	–	4.71
29	F	57	8	Definite	–	–	4.66
30	M	40	28	Definite	–	–	4.63

ALS Amytrophic lateral sclerosis; *CSF* cerebrospinal fluid; *y* years; *m* months; *M* male; *F* female

[a] Patients were diagnosed as "definite" or "probable" ALS according to the revised Al Escorial criteria [3]

[b] Patients 1, 2, 3, 4, 5 and 6 showed higher levels of CSF TDP-43 than the 95% upper confidence level for the control group (>7.18 ng/ml)

were washed three times with PBST [0.01 M phosphate buffer, 0.0027 M potassium chloride and 0.137 M sodium chloride, pH 7.4 (PBS) containing 0.05% Tween 20], and incubated with 200 µl/well of blocking buffer (PBST containing 2.5% gelatin) for 2 h at 37°C. The plates were again washed three times with PBST and 100 µl of the CSF samples to be tested were added to each well. To eliminate inter-assay variability as a confounding factor, all CSF samples were run in duplicate on the same day with the same lot of standards. After washing three times with PBST, the detection antibody, anti-TDP-43 rabbit polyclonal antibody (10782-2-AP, ProteinTech Group, Chicago, USA), 100 µl/well, diluted to 0.2 µg/ml in blocking buffer, was added and the plates were incubated at 37°C for 2 h. After washing three times with PBST, the plates were incubated with 100 µl/well of goat anti-rabbit secondary antibody coupled to horseradish peroxidase (HRP) (Dako Ltd., Denmark), diluted 1:10,000 in blocking buffer, at 37°C for 1 h. After washing four times with PBST, 100 µl/well of an enhanced chemiluminescent substrate (SuperSignal ELISA Femto Maximum Sensitivity Substrate, Pierce Biotechnology, Rockford, USA) was finally added, and then chemiluminescence in relative light units was immediately measured at 395 nm with a microplate luminometer (SpectraMax L, Molecular Device, Tokyo). The standard curve for the ELISA assay was carried out with triplicate measurements using 100 µl/well of recombinant TDP-43 protein (MW 54.3 kDa, AAH01487, recombinant protein with GST tag, Abnova Corporation, Walnut, USA) solution at different concentrations (0.24, 0.48, 0.97, 1.9, 3.9, 7.8, 15.6, 31.2, 62.5, 125 and 250 ng/ml) of the protein in PBS. The relative concentration estimates of CSF TDP-43 were calculated according to each standard curve.

Immunoprecipitation of TDP-43 from CSF

According to the ELISA results, CSF samples from selected patients with SALS giving a high chemiluminescence signal were chosen for immunoprecipitation. One milliliter of the CSF sample, to which a cocktail of protease inhibitors (Calbiochem, San Diego, USA) had been added, was incubated with 10 μg of anti-TDP-43 monoclonal antibody (H00023435-M01, clone 2E2-D3, Abnova Corporation) overnight at 4°C. The resultant solution was immunocaptured with magnetic beads coupled with primary anti-mouse IgG antibodies (Dynabeads sheep anti-mouse IgG, Dynal Biotech Ltd., Wirral, UK), as described by the manufacturer. The beads were then washed three times with PBS. Any captured TDP-43 was eluted from the beads by boiling in Laemmli sample buffer (Bio-Rad, Tokyo, Japan) for 5 min, and examined by gel electrophoresis and immunoblotting.

Gel electrophoresis and immunoblotting

Proteins eluted from the magnetic beads were separated on 10% Tris–glycine polyacrylamide gels (READY GEL J, Bio-Rad, Tokyo, Japan). For immunoblotting, proteins separated by SDS-PAGE were transferred to Immobilon™ Transfer PVDF Membrane (0.45 μm, Millipore, Bedford, USA). The membrane was blocked with 5% dried skimmed milk in 10 mM Tris–HCl, 150 mM NaCl, 0.05% Tween 20, pH 7.5 (TBS-t) overnight at 4°C. After blocking, the membrane was incubated for 2 h with anti-TDP-43 rabbit polyclonal antibody (10782-2-AP, ProteinTech Group, Chicago, USA) diluted to 1:1,000 in TBS-t. The membranes were washed three times in TBS-t, followed by incubation with a secondary antibody, HRP-conjugated goat anti-rabbit antibody (Dako LTD., Denmark), (1:10,000). The protein bands were visualized by using ECL plus (GE healthcare, Little Chalfont, UK) as described by the manufacturer.

Statistical analysis

Regarding differences between the SALS and control groups, the groups were compared using Mann–Whitney *U* test. The level of significance was set at $p < 0.05$. All analyses were carried out using GraphPad Prism software (GraphPad Prism Version 4.0, GraphPad software, San Diego, USA).

Results

Figure 1 shows the standard curve obtained with our ELISA system, demonstrating that TDP-43 was detected with high sensitivity. The goodness of fit was 99.7% and the lower detection limit of the method was 0.49 ng/ml. The intra-assay coefficient of variation (CV) was 9.9% at a concentration of 15.6 ng/ml ($n = 6$), 5.0% at a concentration of 7.8 ng/ml ($n = 6$) and 10.2% at a concentration of 1.95 ng/ml ($n = 6$). The inter-assay CV was 10.7% at a concentration of 15.6 ng/ml ($n = 3$), 6.6% at a concentration of 7.8 ng/ml ($n = 3$) and 10.2% at a concentration of 1.95 ng/ml ($n = 3$).

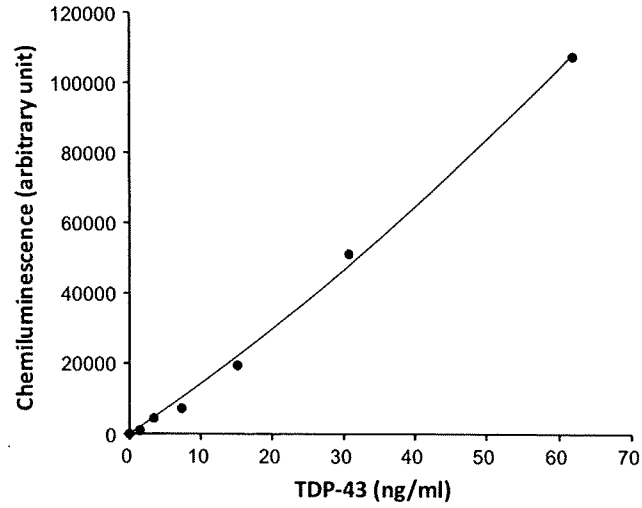

Fig. 1 Standard curve for the TDP-43 ELISA. Data represent the mean ± SD of triplicate readings. The goodness of fit was 99.7% and the lower detection limit of the method was 0.49 ng/ml

In the previous report by Foulds et al., TDP-43 was barely detectable by ELISA in the plasma samples obtained from the vast majority (92%) of healthy control subjects, 77% of patients with AD, and 54% of patients with FTD [9]. Here, we have improved the sensitivity of their ELISA system, with slight modifications based on the use of chemiluminescence for the detection of HRP-labeled reaction, and we could readily determine the concentrations of TDP-43 in human CSF samples. Comparison of the concentrations of TDP-43 in CSF shows that it was significantly higher in the SALS group (mean ± SD 6.92 ± 3.71 ng/ml, $n = 30$) than that in the age-matched control subjects (5.31 ± 0.94 ng/ml, $n = 29$) ($p = 0.023$, Mann–Whitney *U* test; Fig. 2a). As shown in Fig. 2a (dashed line), we estimated the 95% upper confidence level for the control group to be 7.18 ng/ml of TDP-43. Among the 30 patients with SALS, there were six patients (20%) with levels of TDP-43 in CSF higher than this 95% upper confidence limit for the controls (i.e. more than 7.18 ng/ml, Table 1). Interestingly, all of the six patients with higher levels of CSF TDP-43 were examined within 10 months of the onset of illness (Table 1). Among the 30 patients with ALS examined in this study, the patients examined within 10 months of onset showed significantly higher levels of

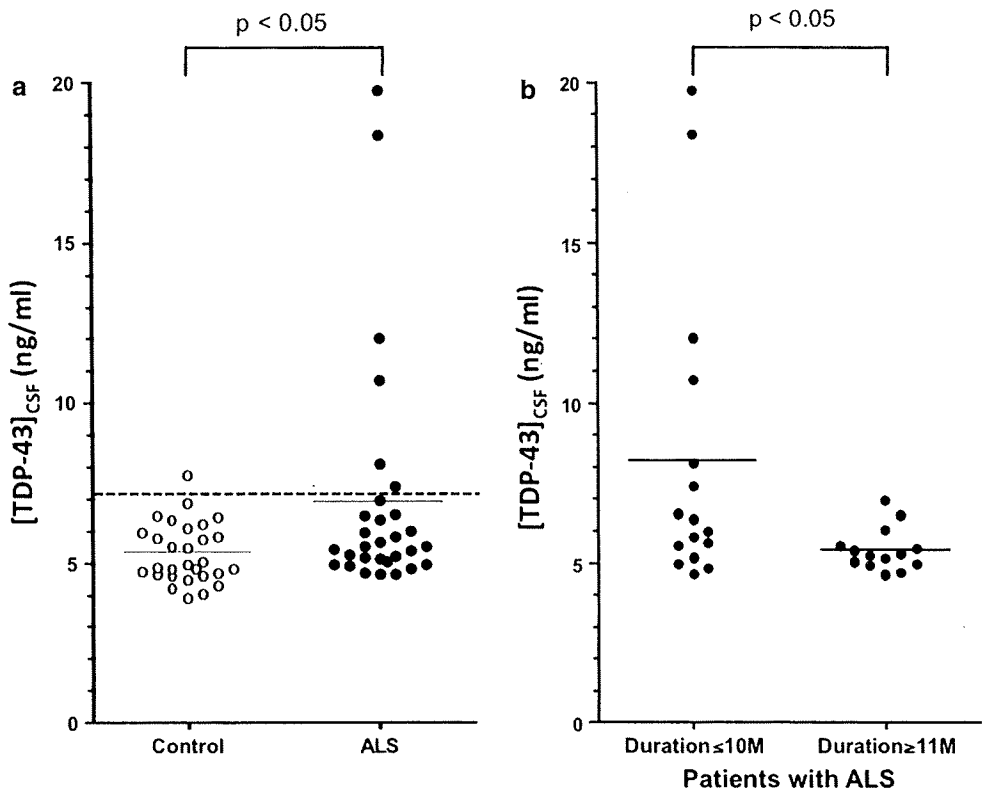

Fig. 2 **a** Plots for the concentrations of TDP-43 in CSF in the control patients ($n = 29$) and the patients with SALS ($n = 30$). The *solid line* represents the mean values of the concentrations of each group. The concentration of CSF TDP-43 in the SALS group was significantly higher than that in the age-matched control subjects ($p = 0.023$, Mann–Whitney U test). The *dashed line* corresponds to the 95% upper confidence level for the control group (7.18 ng/ml). **b** Plots for the concentrations of TDP-43 in CSF in the ALS patients examined within 10 months of onset (duration $\leq$ 10 M, $n = 16$) and those examined after 11 months or more of onset (duration $\geq$ 11 M, $n = 14$). The former showed significantly higher levels of CSF TDP-43 than the latter ($p = 0.028$, Mann–Whitney U test)

CSF TDP-43 (mean ± SD 8.24 ± 4.72 ng/ml, $n = 16$), compared with those examined after 11 months or more of onset (5.41 ± 0.66 ng/ml, $n = 14$) ($p = 0.028$, Mann–Whitney U test; Fig. 2b). These results suggest that the levels of TDP-43 in CSF may increase in the early stage of ALS. Among the six patients with higher levels of CSF TDP-43, five patients were diagnosed as "definite" ALS and four patients had bulbar signs (Table 1). However, not all of the patients with "definite" ALS or with bulbar signs showed an increased concentration of TDP-43 in CSF (Table 1). There were no significant differences in the levels of CSF TDP-43 between "definite" and "probable" ALS groups, as well as between patients with and without bulbar signs (data not shown). There were no significant correlations between the CSF TDP-43 levels and the age of the subjects, for either the SALS or the control groups. Also, there were no significant differences in the levels of CSF TDP-43 between the healthy controls and the disease controls (data not shown).

When proteins in the CSF samples from SALS patients with high levels of TDP-43 (based on ELISA results) were immunocaptured with the anti-TDP-43 monoclonal antibody, and then probed with the anti-TDP-43 rabbit polyclonal antibody on immunoblots, a protein band migrating at ~43 kDa was seen (Fig. 3, lane 2–4). A weaker band at ~43 kDa, migrating in the same place as that in patients with SALS, was detected in a similarly treated low-reading

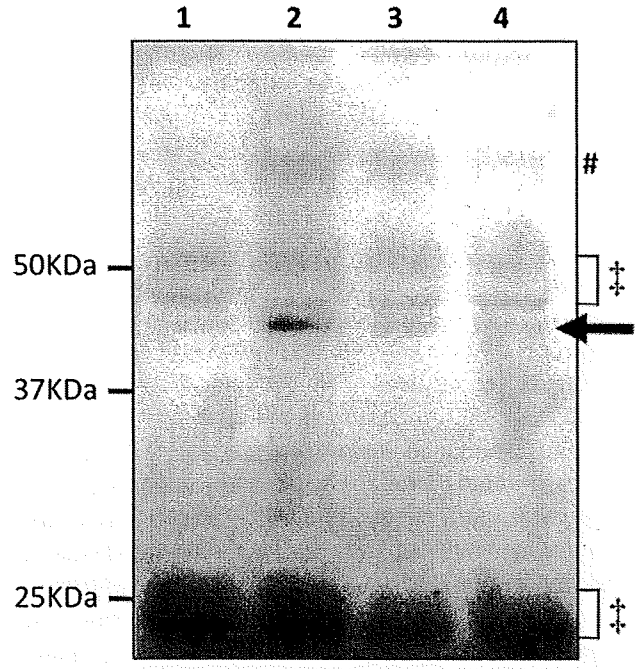

Fig. 3 Immunoblotting of the proteins immunocaptured from CSF samples obtained from a control patient (*lane 1*), and three patients with SALS (*lanes 2–4*) and high ELISA results. TDP-43 is seen as a single band migrating at ~43 kDa (*arrow*). There are also bands present that reacted with the secondary (goat anti-rabbit) antibody, migrating at ~23 and ~50 kDa, which are derived from immunoglobulins (*double dagger*), and those migrating at ~66 kDa derived from albumin (*hash*)

sample obtained from a control subject (Fig. 3, lane 1). The antibodies employed here for the immunocapture and detection by immunoblotting were exactly the same as those used as capture and the reporter antibodies, respectively, in our ELISA system for TDP-43. Using this pair of antibodies, we detected only the ~43 kDa band corresponding to the full-length TDP-43, and did not detect any lower molecular weight bands including ~25 kDa bands corresponding to C-terminal fragments of TDP-43.

Discussion

To our knowledge, this is the first study to report the detection and levels of TDP-43 in human CSF. Further, we also believe that ours is the first study to suggest that CSF TDP-43 concentrations are significantly increased in some patients with SALS as compared with those from age-matched control patients. These measurements were made using ELISA, and the presence of TDP-43 in CSF was confirmed by immunoblotting analysis of the proteins immunocaptured from the CSF samples. Similar results were obtained in an independent study carried out at Lancaster University, though based upon fewer CSF samples. Using the previously published TDP-43 ELISA method [9], 8 CSF samples obtained from Royal Preston Hospital (with local ethical committee approval) were assayed. These comprised samples from two normal individuals, two patients with SALS, and four patients with other neurological disorders. Among these 8 samples, those from the two patients with SALS gave the highest signals (data not shown).

The TDP-43 normally exists and subserves its functions in the nucleus [4, 23] and so is generally considered to be an intracellular protein that is not secreted into the extracellular space. It has, however, been reported recently that TDP-43 can be detected within plasma of some patients with FTD and AD, and also within (fewer) normal controls by using ELISA and immunoblotting analysis [9]. This previous report confirmed the specificity of the antibody pair employed here for the sandwich ELISA, and showed that the readout from the ELISA accurately reflects the levels of TDP-43 present in plasma, as detected by immunoblotting. We used a slightly modified ELISA system, in which the same antibody pair as the previous study, but with a chemiluminescence system for signal detection was used, and we determined the levels of CSF TDP-43 in patients with SALS, during life. Using the same pair of the capture and detection antibodies for immunoblotting analysis of the proteins immunocaptured from CSF, we detected only one specific band (at 43 kDa) corresponding to full-length TDP-43, and did not detect any C-terminal fragments of TDP-43. These results imply that the ELISA system employed in this study predominantly measures the full-length TDP-43 protein.

We suggest that CSF TDP-43 levels are likely to reflect the TDP-43 content of the interstitial and extracellular compartments within the CNS and that the protein is, accordingly, principally of neural origin, possibly including both neuronal and glial cells [20, 35]. A recent report has linked the presence of TDP-43 inclusions to the breakdown of neurons, rather than glial cells: neuronophagia in the SALS spinal cord was found to involve motor neurons containing TDP-43 inclusions, while no motor neurons without TDP-43 inclusions were seen to undergo neuronophagia [24]. This suggests that extracellular TDP-43 in brain and CSF could arise from the degeneration of motor neurons. Normal diffusion through the brain parenchyma as a result of normal cerebral blood flow or extravasation of blood products due to a leaking blood brain barrier is another possible source of TDP-43 in CSF, as TDP-43 is ubiquitously expressed [4] and is found in blood plasma [9]. If the CSF TDP-43 we have detected is of neural rather than peripheral origin, then our findings could reflect a breakdown of affected motor neurons, and correlate with previous pathological studies that have shown that TDP-43 can redistribute from the nucleus to the cytoplasm in affected neurons [6, 19]. Our finding that CSF TDP-43 levels are increased in some patients with SALS, especially in their early stages, shows striking parallels with the growing literature on increased concentrations of tau protein in the CSF of patients with AD and, even more so in Creutzfeldt–Jakob disease, where the level of CSF tau reflects the degree of neuronal degeneration or damage [22, 33].

In this study, 6 of the 30 (20%) SALS patients had CSF TDP-43 levels that exceed the upper 95% confidence limit for the control patients. In the previous study on human plasma, 46% of the FTD and 22% of the AD patients had TDP-43 levels above the upper 99% confidence limit of the reference population [9]. The authors argued that the proportion of patients showing high plasma TDP-43 levels in both FTD and AD closely matched those proportions predicted from histological studies to have ubiquitin/TDP-43-based histology [5, 6, 15, 18, 30]. Histological studies of ALS patients have reported ubiquitin/TDP-43-based pathological changes in almost all non-SOD1 associated patients [16, 20]. The discrepancy between the reported incidence of ubiquitin/TDP-43-based histology in ALS and the percentage of the SALS patients with increased levels of CSF TDP-43 by this study could be explained by one or more of the following hypotheses: (1) some of the control patients might have as yet unidentified reasons to have increased CSF TDP-43 levels. This possibility, however, is unlikely because there was no significant difference in the levels of CSF TDP-43 between the healthy normal controls and the disease controls; (2) elevated levels of CSF TDP-43 might

be observed only in patients with more widespread extramotor and cortical TDP-43 pathology, who accounts for only a small proportion (25–30%) of non-demented patients with SALS [20]. In this study, four out of six SALS patients with increased levels of CSF TDP-43 had bulbar signs, suggesting that those four patients might have more widespread pathology than those without bulbar signs. However, there were also SALS patients with CSF TDP-43 levels similar to the control in spite of positive bulbar signs; (3) CSF TDP-43 levels might depend on the stage of the disease, or rate of disease progression or severity. Regarding the last possibility, our results suggest that the levels of TDP-43 in CSF may be increased in the early stage of ALS, because all of the six patients with increased CSF TDP-43 were examined within 10 months of the onset of disease, and the patients examined within 10 months of onset showed significantly higher levels of CSF TDP-43 than those examined after 11 months or more of onset. If CSF TDP-43 is mainly derived from the breakdown of affected motor neurons, as discussed above, then the levels of CSF TDP-43 in ALS would be increased in the early stage of the disease, reflecting neuronal damage, but might decrease as the disease progresses because this would be accompanied by a decrease in the number of motor neurons in the spinal cord, which are possibly the source of the extracellular TDP-43. Besides, previous studies have shown that the rate of disease progression in ALS varies at different stages of the disease in the same patient [12], and that TDP-43 pathology found in SALS of long duration was apparently mild in degree and limited in distribution [21]. Further longitudinal studies based on repeat sampling from the same ALS patients in the different stages of the disease will help to address this matter.

Foulds et al. showed that TDP-43 is constitutively released into the extracellular space and could be detected in plasma [9]. Our results have also demonstrated that the levels of TDP-43 in CSF could be determined in living patients by using a sensitive ELISA, and that these levels may be increased in the early stage of ALS. Although we recognize that the present data are still very preliminary, our findings suggest that the quantification of TDP-43 in CSF or peripheral plasma (or both) could have potential value as diagnostic laboratory tools for patients with TDP-43 proteinopathies, such as FTLD-U and ALS, especially the early stages of ALS. No biological marker reflective of this kind of pathology is available for any of these disorders. Besides, from the point of view of genetics, the expression levels of TDP-43 in CSF and plasma are particularly important in ALS, because the recent discovery of pathogenic missense mutations in the *TARDBP* gene in FALS and SALS cases, none of whom had evidence of FTLD, demonstrates that defects in the *TARDBP* gene are sufficient to cause some part of FALS and SALS [10, 13, 31, 34]. The sensitivity and usefulness of TDP-43 as a biomarker in clinical practice could be improved by developing ELISA systems that are more specific for pathological forms of TDP-43, including phosphorylated TDP-43 and its N- or C-terminal fragments. Large-scale, prospective, and well-controlled studies, especially those that include subjects with autopsy-confirmed ALS with TDP-proteinopathy, are necessary to validate the usefulness of quantification of normal or pathological forms of TDP-43 as an urgently needed surrogate marker for the diagnosis and disease progression of ALS.

Acknowledgments This work was supported by Grant-in-Aid from the Research Committee of CNS Degenerative Disease, the Ministry of Health, Labor, and Welfare of Japan (to M.N.) and by Grant-in-Aid for Scientific Research (C) (20591007), the Ministry of Education, Culture, Sports, Science and Technology and Japan Society for the Promotion of Science (to T.T.). P.F. is supported by a grant from The Medical Research Council, UK.

References

1. Abe K, Fujimura H, Toyooka K, Sakoda S, Yorifuji S, Yanagihara T (1997) Cognitive function in amyotrophic lateral sclerosis. J Neurol Sci 148:95–100. doi:10.1016/S0022-510X(96)05338-5
2. Arai T, Hasegawa M, Akiyama H et al (2006) TDP-43 is a component of ubiquitin-positive tau-negative inclusions in frontotemporal lobar degeneration and amyotrophic lateral sclerosis. Biochem Biophys Res Commun 351:602–611. doi:10.1016/j.bbrc.2006.10.093
3. Brooks BR, Miller RG, Swash M, Munsat TL, World Federation of Neurology Research Group on Motor Neuron Diseases (2000) El Escorial revisited: revised criteria for the diagnosis of amyotrophic lateral sclerosis. Amyotroph Lateral Scler Other Motor Neuron Disord 1:293–299. doi:10.1080/146608200300079536
4. Buratti E, Dörk T, Zuccato E, Pagani F, Romano M, Baralle FE (2001) Nuclear factor TDP-43 and SR proteins promote in vitro and in vivo CFTR exon 9 skipping. EMBO J 20:1774–1784. doi:10.1093/emboj/20.7.1774
5. Cairns NJ, Bigio EH, Mackenzie IR, Consortium for Frontotemporal Lobar Degeneration et al (2007) Neuropathologic diagnostic and nosologic criteria for frontotemporal lobar degeneration: consensus of the Consortium for Frontotemporal Lobar Degeneration. Acta Neuropathol 114:5–22. doi:10.1007/s00401-007-0237-2
6. Cairns NJ, Neumann M, Bigio EH et al (2007) TDP-43 in familial and sporadic frontotemporal lobar degeneration with ubiquitin inclusions. Am J Pathol 171:227–240. doi:10.2353/ajpath.2007.070182
7. Davidson Y, Kelley T, Mackenzie IR et al (2007) Ubiquitinated pathological lesions in frontotemporal lobar degeneration contain the TAR DNA-binding protein, TDP-43. Acta Neuropathol 113:521–533. doi:10.1007/s00401-006-0189-y
8. Dickson DW, Josephs KA, Amador-Ortiz C (2007) TDP-43 in differential diagnosis of motor neuron disorders. Acta Neuropathol 114:71–79. doi:10.1007/s00401-007-0234-5
9. Foulds P, McAuley E, Gibbons L et al (2008) TDP-43 protein in plasma may index TDP-43 brain pathology in Alzheimer's disease and frontotemporal lobar degeneration. Acta Neuropathol 116:141–146. doi:10.1007/s00401-008-0389-8
10. Gitcho MA, Baloh RH, Chakraverty S et al (2008) TDP-43 A315T mutation in familial motor neuron disease. Ann Neurol 63:535–538. doi:10.1002/ana.21344

11. Gros-Louis F, Gaspar C, Rouleau GA (2006) Genetics of familial and sporadic amyotrophic lateral sclerosis. Biochim Biophys Acta 1762:956–972
12. Guiloff RJ, Goonetilleke A (1995) Natural history of amyotrophic lateral sclerosis. Observations with the Charing Cross Amyotrophic Lateral Sclerosis Rating Scales. Adv Neurol 68:185–198
13. Kabashi E, Valdmanis PN, Dion P et al (2008) TARDBP mutations in individuals with sporadic and familial amyotrophic lateral sclerosis. Nat Genet 40:572–574. doi:10.1038/ng.132
14. Kwong LK, Neumann M, Sampathu DM, Lee VM, Trojanowski JQ (2007) TDP-43 proteinopathy: the neuropathology underlying major forms of sporadic and familial frontotemporal lobar degeneration and motor neuron disease. Acta Neuropathol 114:63–70. doi:10.1007/s00401-007-0226-5
15. Lipton AM, White CL 3rd, Bigio EH (2004) Frontotemporal lobar degeneration with motor neuron disease-type inclusions predominates in 76 cases of frontotemporal degeneration. Acta Neuropathol 108:379–385. doi:10.1007/s00401-004-0900-9
16. Mackenzie IR, Bigio EH, Ince PG et al (2007) Pathological TDP-43 distinguishes sporadic amyotrophic lateral sclerosis from amyotrophic lateral sclerosis with SOD1 mutations. Ann Neurol 61:427–434. doi:10.1002/ana.21147
17. Mercado PA, Ayala YM, Romano M, Buratti E, Baralle FE (2005) Depletion of TDP 43 overrides the need for exonic and intronic splicing enhancers in the human apoA-II gene. Nucleic Acids Res 33:6000–6010. doi:10.1093/nar/gki897
18. Mott RT, Dickson DW, Trojanowski JQ et al (2005) Neuropathologic, biochemical, and molecular characterization of the frontotemporal dementias. J Neuropathol Exp Neurol 64:420–428
19. Neumann M, Sampathu DM, Kwong LK et al (2006) Ubiquitinated TDP-43 in frontotemporal lobar degeneration and amyotrophic lateral sclerosis. Science 314:130–133. doi:10.1126/science.1134108
20. Nishihira Y, Tan CF, Onodera O et al (2008) Sporadic amyotrophic lateral sclerosis: two pathological patterns shown by analysis of distribution of TDP-43-immunoreactive neuronal and glial cytoplasmic inclusions. Acta Neuropathol 116:169–182. doi:10.1007/s00401-008-0385-z
21. Nishihira Y, Tan CF, Hoshi Y et al. (2008) Sporadic amyotrophic lateral sclerosis of long duration is associated with relatively mild TDP-43 pathology. Acta Neuropathol. doi:10.1007/s00401-008-0443-6
22. Otto M, Wiltfang J, Tumani H et al (1997) Elevated levels of tau-protein in cerebrospinal fluid of patients with Creutzfeldt–Jakob disease. Neurosci Lett 225:210–212. doi:10.1016/S0304-3940(97)00215-2
23. Ou SH, Wu F, Harrich D, García-Martínez LF, Gaynor RB (1995) Cloning and characterization of a novel cellular protein, TDP-43, that binds to human immunodeficiency virus type 1 TAR DNA sequence motifs. J Virol 69:3584–3596
24. Pamphlett R, Kum Jew S (2008) TDP-43 inclusions do not protect motor neurons from sporadic ALS. Acta Neuropathol 116:221–222. doi:10.1007/s00401-008-0392-0
25. Pasinelli P, Brown RH (2006) Molecular biology of amyotrophic lateral sclerosis: insights from genetics. Nat Rev Neurosci 7:710–723. doi:10.1038/nrn1971
26. Piao YS, Wakabayashi K, Kakita A et al (2003) Neuropathology with clinical correlations of sporadic amyotrophic lateral sclerosis: 102 autopsy cases examined between 1962 and 2000. Brain Pathol 13:10–22
27. Ringholz GM, Appel SH, Bradshaw M, Cooke NA, Mosnik DM, Schulz PE (2005) Prevalence and patterns of cognitive impairment in sporadic ALS. Neurology 65:586–590. doi:10.1212/01.wnl.0000172911.39167.b6
28. Seelaar H, Schelhaas HJ, Azmani A et al (2007) TDP-43 pathology in familial frontotemporal dementia and motor neuron disease without Progranulin mutations. Brain 130:1375–1385. doi:10.1093/brain/awm024
29. Shaw CE, Al-Chalabi A, Leigh N (2001) Progress in the pathogenesis of amyotrophic lateral sclerosis. Curr Neurol Neurosci Rep 1:69–76. doi:10.1007/s11910-001-0078-7
30. Shi J, Shaw CL, Du Plessis D et al (2005) Histopathological changes underlying frontotemporal lobar degeneration with clinicopathological correlation. Acta Neuropathol 110:501–512. doi:10.1007/s00401-005-1079-4
31. Sreedharan J, Blair IP, Tripathi VB et al (2008) TDP-43 mutations in familial and sporadic amyotrophic lateral sclerosis. Science 319:1668–1672. doi:10.1126/science.1154584
32. Tan CF, Eguchi H, Tagawa A et al (2007) TDP-43 immunoreactivity in neuronal inclusions in familial amyotrophic lateral sclerosis with or without SOD1 gene mutation. Acta Neuropathol 113:535–542. doi:10.1007/s00401-007-0206-9
33. Vigo-Pelfrey C, Seubert P, Barbour R et al (1995) Elevation of microtubule-associated protein tau in the cerebrospinal fluid of patients with Alzheimer's disease. Neurology 45:788–793
34. Yokoseki A, Shiga A, Tan CF et al (2008) TDP-43 mutation in familial amyotrophic lateral sclerosis. Ann Neurol 63:538–542. doi:10.1002/ana.21392
35. Zhang H, Tan CF, Mori F et al (2008) TDP-43-immunoreactive neuronal and glial inclusions in the neostriatum in amyotrophic lateral sclerosis with and without dementia. Acta Neuropathol 115:115–122. doi:10.1007/s00401-007-0285-7